IEEE Access
Multidisciplinary | Rapid Review | Open Access Journal

Received February 11, 2020, accepted March 2, 2020, date of publication March 9, 2020, date of current version March 25, 2020.

Digital Object Identifier 10.1109/ACCESS.2020.2979470

Wavelength- and Intensity-Demodulated Dual-Wavelength Fiber Laser Sensor for Simultaneous RH and Temperature Detection

BIN YIN[1], GUOFENG SANG[1], RAN YAN[1], YUHENG WU[1], SONGHUA WU[1,2], MUGUANG WANG[3], (Member, IEEE), WENQI LIU[4], HAISU LI[3], AND QICHAO WANG[1]

[1]College of Information Science and Engineering, Ocean Remote Sensing Institute, Ocean University of China, Qingdao 266100, China
[2]Laboratory for Regional Oceanography and Numerical Modeling, Pilot National Laboratory for Marine Science and Technology (Qingdao), Qingdao 266237, China
[3]Institute of Lightwave Technology, Beijing Jiaotong University, Beijing 100044, China
[4]Qingdao Institute of Bioenergy and Bioprocess Technology, Chinese Academy of Sciences, Qingdao 266101, China

Corresponding author: Bin Yin (binyin@ouc.edu.cn)

This work was supported in part by the National Key Research and Development Program of China under Grant 2018YFC0213106 and Grant2016YFE0125700, in part by the National Natural Science Foundation of China under Grant 61901429, Grant 61775015, and Grant 61975191, in part by the Natural Science Foundation of Shandong Province under Grant ZR2019BF003, and in part by the Key Laboratory of All Optical Network and Advanced Telecommunication Network, Ministry of Education, Beijing Jiaotong University under Grant AON2019004.

ABSTRACT We report a dual-wavelength fiber laser sensor based on a uniform fiber Bragg grating (UFBG) and a Polyvinyl alcohol (PVA) film-coated long-period grating (LPG) as sensor probe for simultaneous detection of relative humidity (RH) and temperature. Two UFBGs and the LPG were inscribed in three single mode fibers utilizing phase/amplitude mask technology and mobile scanning technique via the 248 nm UV laser. In our experiment, the RH function based on the differential intensity measurement at dual-wavelength output from 30% to 85% is in a quadratic equation, and the RH sensitivity coefficient of 0.358 dB/% shows good linear relationship and stability from 55% to 85%. Meanwhile, the temperature sensitivity coefficients based on wavelength detection and differential intensity detection are 9.1 pm/°C and 0.21 dB/°C, respectively. The structure of dual-wavelength fiber laser sensor with high signal to noise ratio (SNR), narrow spectral width and good stability enables simultaneous measurement of the RH and temperature with high accuracy and good repeatability.

INDEX TERMS Dual-wavelength fiber laser, fiber laser sensor, fiber Bragg grating, long-period grating, relative humidity, temperature.

I. INTRODUCTION

The simultaneous detection of the humidity and temperature has a significant requirement in applications such as meteorological services, biomedical devices, food processing and storage, chemical and electronic processing, and so on [1]–[3]. The relative humidity (RH), which denotes the partial water vapor pressure relative to the saturation water vapor pressure at static temperature, has been widely applied in the humidity sensing [4]. Conventional mechanical and electronic humidity sensors have many limitations such as low sensitivity, long response time, only single parameter measurement. Therefore, the deep investigation of the humidity and temperature sensors with simultaneous measurement, small size, high accuracy, fast response and good repeatability is necessary [5], [6].

The fiber-optic sensors are able to possess the above-mentioned characteristics [7]–[10]. There already exist numerous fiber-optic RH and temperature sensors based on uniform fiber Bragg grating (UFBG) [11], long-period grating (LPG) [12], and different kinds of multimode interferometer [13]. G. Berruti et.al. reported a fiber-optic humidity sensor utilizing polyimide-coated UFBG applied in high-energy physics field below 0°C as same as their radiation hardness capability when exposed to strong ionizing radiations (up to 10 kGy) [14]. Chao-Tsung Ma et. al proposed

The associate editor coordinating the review of this manuscript and approving it for publication was Sukhdev Roy.

a dual-polymer fiber Fizeau interferometer for simultaneous measurement of RH and temperature. The measured RH and temperature sensitivities of two sensors are 0.12538 nm/%, 0.25376 nm/°C, 0.15807 nm/%, and 0.38551 nm/°C [15]. S. N. Wu et. al reported a fiber-optic RH and temperature sensor based on polyvinyl alcohol (PVA)-coated open-cavity Fabry-Perot interferometer (FPI). The highest sensitivity of RH measurement for the reflection loss of FPI from 30% to 90% was −1.2 dB/%, and the sensitivities RH and temperature for the dip wavelength were −23.1 pm/% and −6.14 pm/°C, respectively [16].

Recently, fiber laser has attracted a great deal of attention in the sensing field on account of the superior advantages including high signal to noise ratio (SNR), good stability, and narrow spectral width compared with conventional sensor using broadband light source and so on [17]–[20]. X. C. Yang et. al reported a dual-wavelength ring laser gas sensor using tunable Fabry-Perot filter, hollow-core photonic crystal fiber, and UFBG. The minimum detection limit at 20 s response time was 10.42 ppmV by experiment [21]. Javier A. Martin-Vela et. al presented a fiber laser curvature sensor based on an LPG with the curvature sensitivity of −42.488 nm/m^{-1} [22]. Y. Dai et. al reported a dual-wavelength fiber laser liquid-level sensor based on two parallel phase-shift FBGs and one UFBG. The measured liquid-level sensitivity in the experiment within 1.5 mm range was 2.12 × 107 MHz/m [23].

In this article, we present a wavelength- and intensity-demodulated fiber laser sensor for simultaneous detection of the RH and temperature. Two UFBGs as reflection filter and the PVA-coated LPG as intensity modulation embed into a laser ring cavity achieve stable dual-wavelength lasing and sensing. The resonance peak wavelength shift and differential power intensity change of dual-wavelength laser varied with RH and temperature. In the experiment, the measured SNR, 3dB spectral width and stability of fiber laser are 45 dB, 0.04 nm and <0.1dB (0.02nm), respectively. The RH function based on the differential output power measurement from 30% to 85% is in a quadratic equation, and the measured quadratic and linear coefficients are 0.005 dB/%^{2} and −0.335 dB/%, respectively. From 55% to 85%, the RH function shows good linear relation and the RH sensitivity coefficient is 0.358 dB/%. The temperature function based on lasing wavelength measurement and differential output power measurement all shows a linear relation. Meanwhile, the temperature sensitivity coefficients of 9.1 pm/°C and 0.021 dB/°C are obtained. Based on the measured cross sensitivity coefficients and stability, the RH and temperature accuracy of the fiber laser sensor is calculated as 0.35% and 2.2 °C, which are more than some traditional fiber sensors [24], [25]. Thus, the proposed laser sensor for RH and temperature measurement has high SNR, high accuracy, good repeatability, and low error, which could be applied in chemical, engineering, and biochemical monitoring fields.

II. SENSING PRINCIPLE AND EXPERIMENTAL STRUCTURE

A. SENSING PRINCIPLE

The standard fiber laser sensor structure includes pump source, resonant cavity, gain fiber and other optical modulation elements. As a new kind of the fiber sensor, the fiber laser sensor mainly adopts the resonator cavity or optical filter of the fiber laser as the sensing probe to measure the parameters such as temperature, strain, refractive index and so on by the wavelength, intensity, phase or beat frequency of the fiber laser. In our proposed fiber laser sensor system, the sensing probe includes the $UFBG_2$ and the PVA-coated LPG. The sensing principle of UFBG (including $UFBG_1$ and $UFBG_2$) utilizes the Bragg wavelength shift $\Delta\lambda_{UFBG1,2}$ detection with the variation of axial strain and temperature. The normal UFBG uncoated any material is not sensitive to humidity. Meanwhile, this experiment only analyzes the response of the sensing probe to the temperature and RH. In combination with our experiments, we fixed both ends of the sensing probe in the metal frame to keep the axial strain constant. It made sure that there was no external stimulus acting on the laser sensing probe other than the temperature and RH. Thus, the relationship between $\Delta\lambda_B$ and the variation of temperature ΔT is written as [26]:

$$\Delta\lambda_{UFBG} = \left(\frac{1}{n_{eff}}\xi + \alpha\right) \times \Delta T \tag{1}$$

where ξ and α represent the thermo-optical coefficient and linear thermal expansion coefficient of fiber, respectively. The spectrum of UFBG with the variation of temperature is depicted in Fig. 1(a). If the temperature sensitivity coefficient is assumed to be $K_{11} = \left(\frac{1}{n_{tf}}\xi + \alpha\right)$, the above equation (1) can be abbreviated as

$$\Delta\lambda_{UFBG} = K_{11} \times \Delta T \tag{2}$$

Furthermore, the laser wavelength is the same as the wavelength of UFBG on account of the dual-wavelength fiber laser generated by the reflection of UFBG. Due to $UFBG_2$ as the part of the sensing probe and $UFBG_1$ as the reference grating, the wavelength difference of dual-wavelength fiber laser should be expressed as

$$\begin{aligned}\Delta\lambda_{laser} &= \Delta\lambda_{laser2} - \Delta\lambda_{laser1} = \Delta\lambda_{UFBG2} - \Delta\lambda_{UFBG1} \\ &= \Delta\lambda_{UFBG2} = K_{11} \times \Delta T\end{aligned} \tag{3}$$

Meanwhile, the dual-wavelength output power intensity also varies with the wavelength of UFBG.

The LPG with a period typically in the hundreds of microns promotes coupling between the propagating core mode and co-propagating cladding modes. The high attenuation of the cladding modes leads to the transmission spectrum of the LPG which contains a series of attenuation bands with discrete resonant wavelengths, and each attenuation band corresponds to the coupling to a different cladding mode [27].

The spectral shape and the resonant wavelengths of the attenuation bands are related to the period and length of

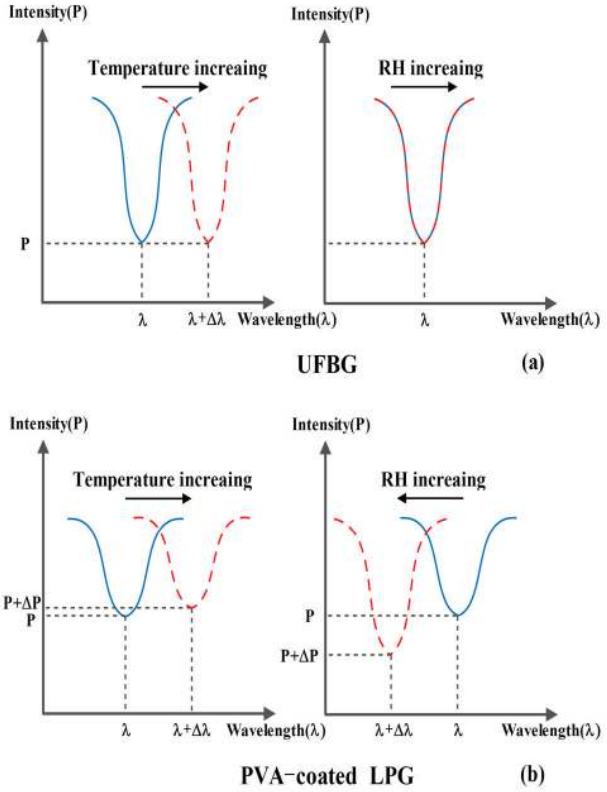

FIGURE 1. (a) Spectral principle of UFBG-based sensors for temperature and RH monitoring. (b) Spectral principle of PVA-coated LPG-based sensors for temperature and RH monitoring.

the LPG, and also sensitive to the ambient environment including temperature, strain, bend radius and refractive index of the medium surrounding. The changes of these parameters can alter the period of the LPG and/or the effective refractive index difference of the core and cladding modes. Furthermore, the phase-matching conditions for coupling to the cladding modes is modified, which results in a variation in the resonant wavelengths and powers of the attenuation bands [28].

The sensitivity to a particular measurand is dependent upon the composition of the fiber and the order of the cladding mode to which the guided optical power is coupled, and is thus different for each attenuation band. These characteristics enable the LPG particularly attractive for sensor applications [29].

Because the change of LPG resonance wavelength results from the influence of RH and temperature, the resonance wavelength shift $\Delta\lambda_{LPG}$ can be expressed as [30]

$$\Delta\lambda_{LPG} = k_{11}\Delta T + k_{12}\Delta RH \tag{4}$$

where k_{11} and k_{12} represent the sensitivity coefficients of temperature and RH in wavelength, respectively. The spectrum of the PVA-coated LPG with the change of the temperature and RH is described in Fig. 1(b). The intensity variation of the PVA-coated LPG in resonance wavelength results from the variation of the RH (ΔRH) and temperature (ΔT) is written as

$$\Delta P_{LPG} = k_{21}\Delta T + k_{22}\Delta RH \tag{5}$$

where k_{21} and k_{23} are the sensitivity coefficients of the temperature and RH in intensity, respectively. Since both temperature and RH will cause variations of the PVA-coated LPG in resonant wavelength and resonant peak intensity, and then the changes of the fiber laser in the peak power intensity will be affected. Meanwhile, the wavelength change of UFBG caused by temperature will also affect the laser output power intensity variation. Thus, the intensity difference variation of the proposed fiber laser output (include the effects of UFBG and PVA-coated LPG) can be expressed as

$$\Delta P_{laser} = K_{21}\Delta T + K_{22}\Delta RH \tag{6}$$

Based on the equation (3) and (6), the coefficient matrix can be given by

$$\begin{bmatrix} \Delta\lambda_{laser} \\ \Delta P_{laser} \end{bmatrix} = \begin{bmatrix} K_{11} & 0 \\ K_{21} & K_{22} \end{bmatrix} \begin{bmatrix} \Delta T \\ \Delta RH \end{bmatrix} \tag{7}$$

The variation of temperature and RH by matrix transformation can be expressed as

$$\begin{bmatrix} \Delta T \\ \Delta RH \end{bmatrix} = \frac{1}{D} \begin{bmatrix} K_{22} & 0 \\ -K_{21} & K_{11} \end{bmatrix} \begin{bmatrix} \Delta\lambda_{laser} \\ \Delta P_{laser} \end{bmatrix} \tag{8}$$

where $D = K_{11}K_{22}$, K_{11}, K_{21}, K_{22} can be determined by measured curve based on temperature and RH responses separately for $\Delta\lambda_{laser}$ and ΔP_{laser} [31]. According to the above analysis, the variations of the temperature and RH can be evaluated by expression (8).

B. FABRICATION PROCESS

Two UFBGs and the LPG were separately fabricated in three 10-day hydrogen-loaded (10 Mpa; at room temperature) B/Ge co-doped single mode fibers (the length is about 30 cm) using phase/amplitude mask technology and mobile scanning technique, exposed by the 248 nm UV laser with 80 mJ pulse energy and 10 Hz pulse frequency. The fabrication and schematics are shown in Fig. 2. The periods of the phase mask are 1068 nm for $UFBG_1$ and 1075 nm for $UFBG_2$, and the period of the amplitude mask is 250 μm. The length of two UFBGs is respectively 1.0 cm, and the length of the LPG is about 2.0 cm. Fig. 3(b) displays the measured transmission spectrum of the fabricated UFBGs and LPG from 1540 nm to1570 nm. Through the analysis of data, the center wavelengths of UFBGs are 1543.7 nm and 1558.04 nm, respectively. Two UFBGs and the LPG were annealed at 18 °C for 8 h before being ready for employing in the experiments. Then, the LPG and $UFBG_2$ are fused together with a cutting knife and a fusion splicer as the sensor probe, and $UFBG_1$ is fused into the laser ring as a reference grating.

In order to coat the LPG, the PVA solution should first be prepared. In our experiment, the PVA (PVA-205, low viscosity) was supplied by Aladdin company. The configuration process of 3% PVA aqueous solution is as follows (take 3% as an example). Firstly, 3 g low-viscosity PVA granules for

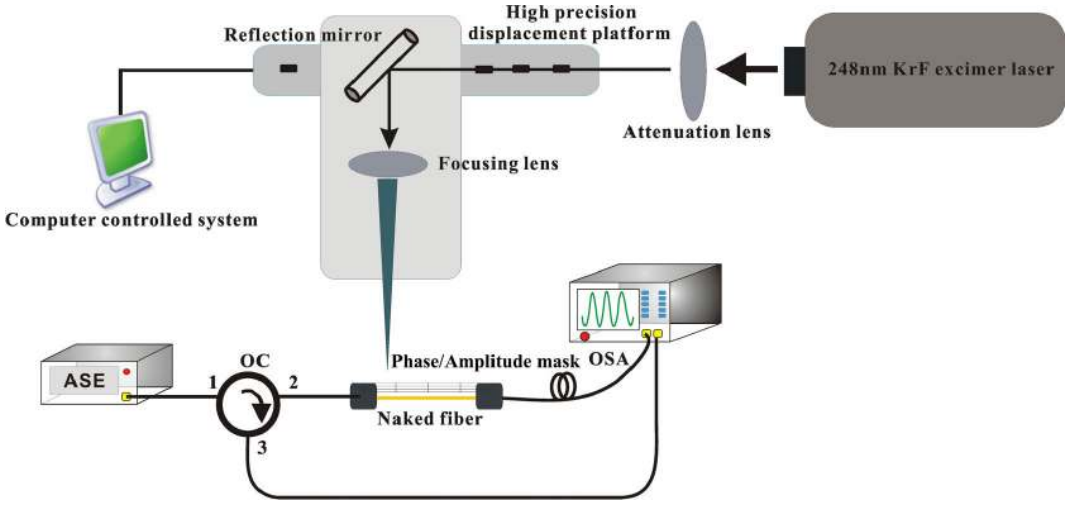

FIGURE 2. The fabrication and schematics of the LPG and UFBG (including $UFBG_1$ and $UFBG_2$).

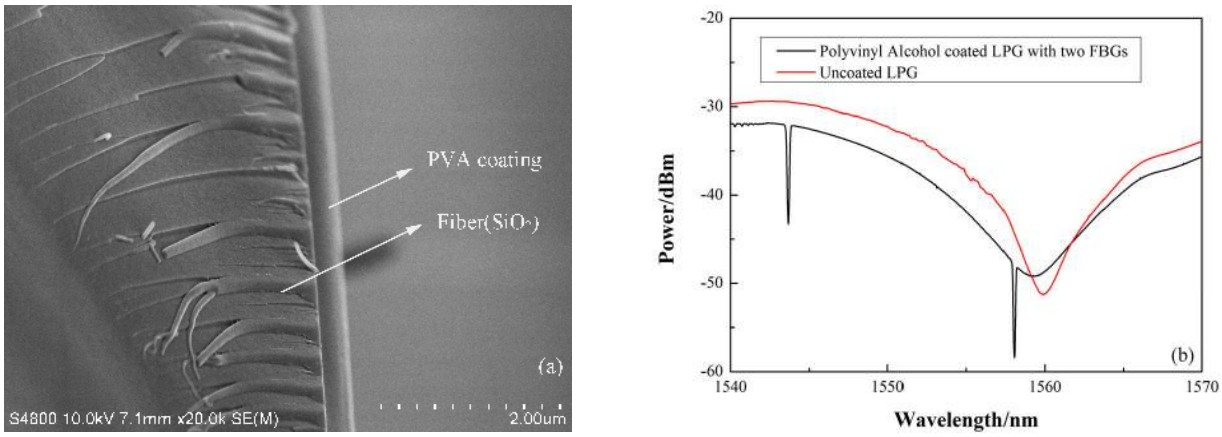

FIGURE 3. (a) The image of PVA-coated LPG at the scanning electron microscope; (b) Transmission spectrum of the uncoated LPG (red line) and the PVA-coated LPG with two UFBGs (black line).

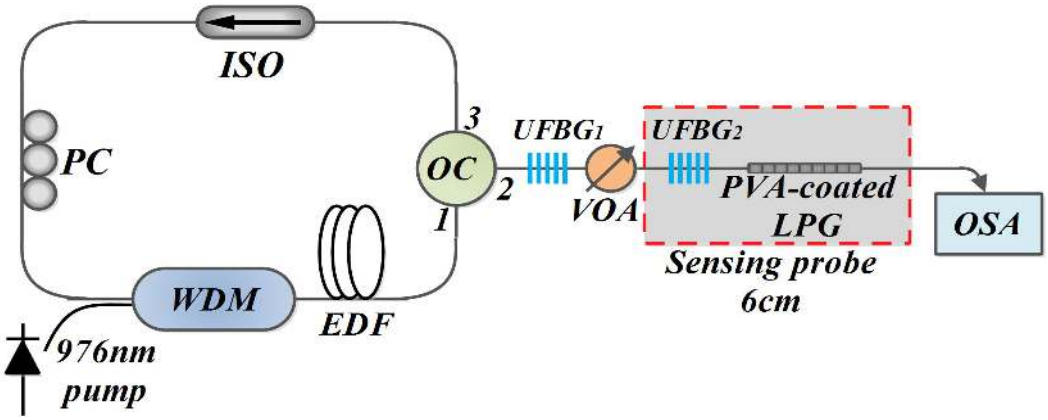

FIGURE 4. Experimental structure diagram of the proposed fiber laser sensor using PVA-coated LPG and dual UFBG.

several times (about 0.5 g each time) were dissolved into 97 g deionized water at 90 °C with magnetic stirring for 30 minutes. Then, the aqueous solutions were taken into a climate chamber with keeping temperature 90∼95 °C for 2 h until complete alcoholysis. The fabricated LPG was cleaned with deionized water and evaporated in the air, repeatedly. Then, The LPG was fully immersed into the PVA aqueous solution for coating 1 h at 80 °C by using the dip-coating

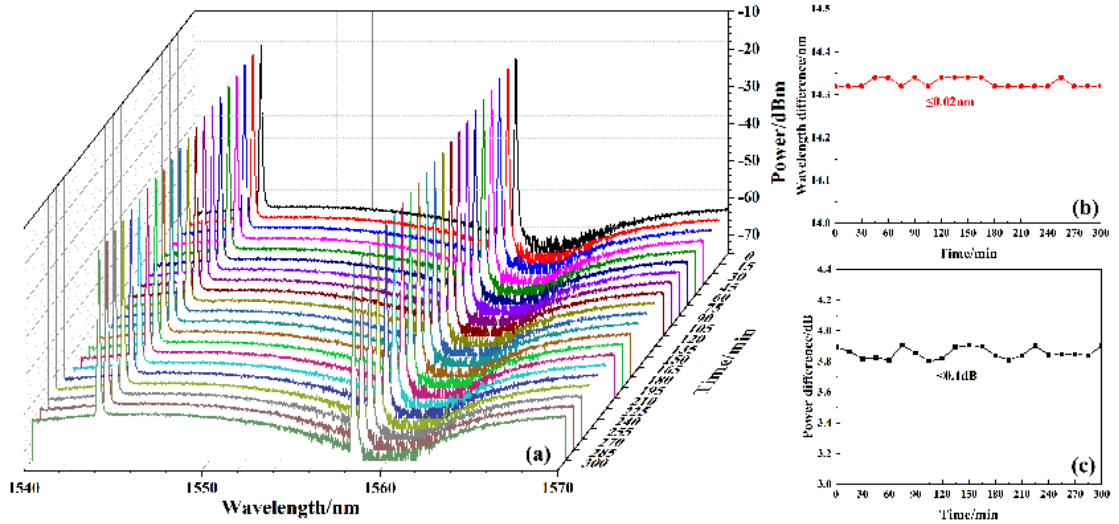

FIGURE 5. (a) Measured output spectra of dual-wavelength fiber laser sensor based on the PVA-coated LPG and dual UFBG at 15 minutes interval during five hours. (b) (c) The variation of lasing output power intensity and wavelength during five hours.

process. At last, the PVA-coated LPG was dried in the climate chamber for 1 h at 50 °C to evaporated off the water of the LPG surface. The image of the PVA-coated LPG at the scanning electron microscope is shown in Fig. 3(a).

C. EXPERIMENTAL STRUCTURE

The experimental structure diagram of the proposed fiber ring laser sensor is depicted in Fig. 4. A 3 m long erbium-doped fiber (EDF, YOFC-ED1016, absorption of 36 dB/m, the peak of which is at 1532 nm) is used as a gain medium. The pumped light from 976 nm laser diode enters the gain medium through 980/1550 nm wavelength division multiplexer (WDM). A 3-port optical circulator (OC) united with dual UFBGs ($UFBG_1\lambda_1 = 1543.7$ nm, $UFBG_2\lambda_2 = 1558.04$ nm) is used to reflect the dual-channel lasing light into the ring cavity. An optical isolator is inserted in the ring cavity in order to assure the unidirectional operation and prevent any negative effects such as spatial hole burning. Furthermore, the PVA-coated LPG cascaded with $UFBG_2$ as an integrated sensing probe is used to achieve the perception of the RH and temperature change. Meanwhile, the distance between the PVA-coated LPG and $UFBG_2$ is limited to centimeter magnitude to ensure the sensing probe in the same measurement environment. The other port of the sensing probe is connected with an optical spectrum analyzer (OSA, 0.1 nm resolution). The sensing probe (the length of 6 cm) is put into the climate chamber for realizing to monitor the changes of RH and temperature. Through measuring the output spectrum (wavelength and differential power intensity) of the proposed fiber laser sensor system by OSA, the simultaneous detection of the RH and temperature with high accuracy and good repeatability is achieved.

III. EXPERIMENT RESULTS AND DISCUSSIONS

A. LASER OUTPUT CHARACTERISTIC

The fiber laser can immensely improve the performance of the fiber sensor on account of their high SNR, high stability

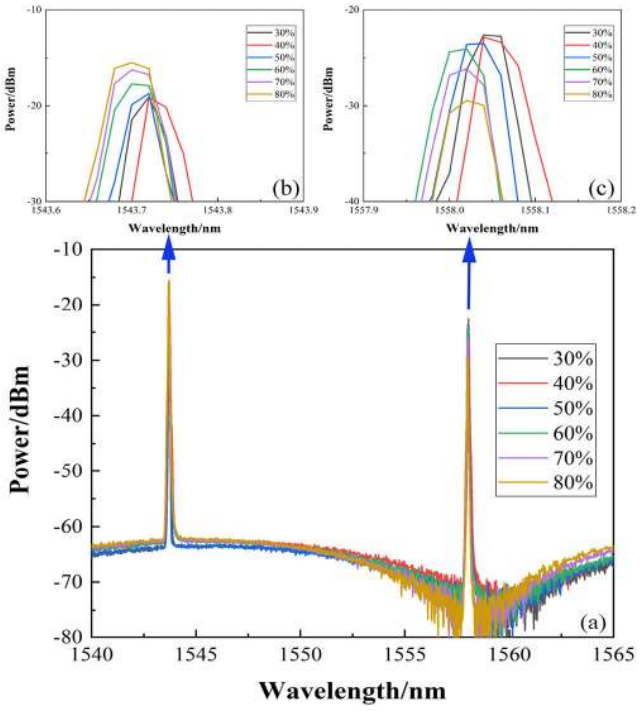

FIGURE 6. (a) Measured output spectral of the proposed dual-wavelength fiber laser sensor under different RH (from 30% to 80%); (b)(c) Local amplification diagram of laser peak location.

and narrow spectral width [32]. In our experiment, the pump light was set at 248 mW which was beyond the pump threshold 150 mW. Through adjusting the polarization controller (PC) and variable optical attenuator (VOA), the stable dual-wavelength lasing was achieved. Fig. 5(a) shows the measured output spectra of the proposed dual-wavelength fiber laser sensor with dual UFBGs and the PVA-coated LPG scanned repeatedly at 15 minutes interval in five hours. From the measured output spectra, we can find that the dual-line laser emission which is slightly greater than the Bragg

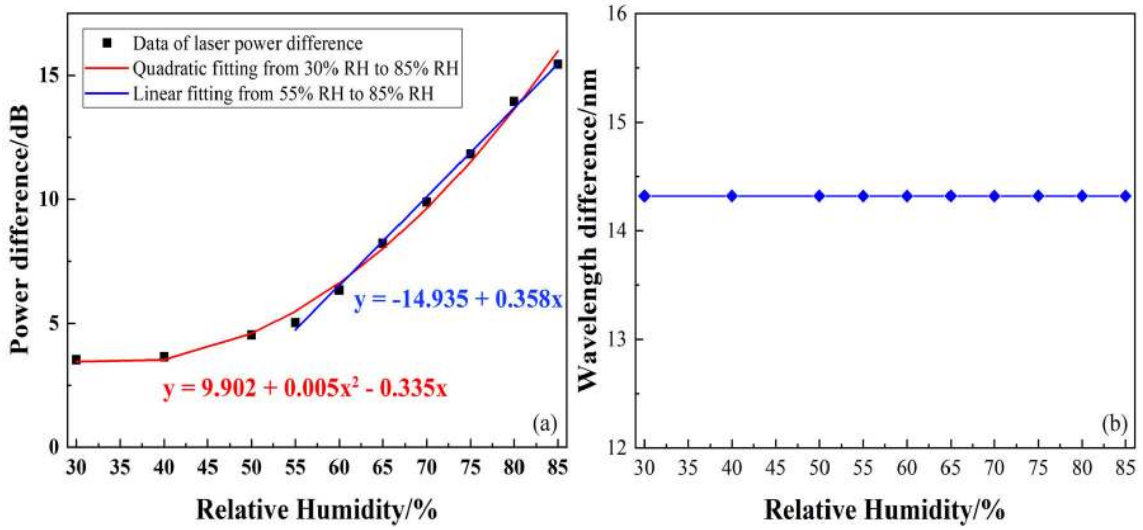

FIGURE 7. (a) The differential intensity variation of dual-wavelength laser sensor as a function of RH. (b) The wavelength difference variation of proposed laser sensor along with the surrounding RH.

wavelengths of dual UFBGs is generated at 1543.74 nm and 1558.08 nm with SNR of 45 dB and 3dB bandwidth of 0.04 nm. Additionally, the wavelength and power stability of the dual-wavelength fiber laser at room temperature is validated as shown in Fig.5. From Fig. 5(b) and 5(c), the maximum variations of lasing power intensity and lasing wavelength are less than 0.1 dB and 0.02 nm, respectively. By the stability study above, the high SNR, high stability and narrow spectral width performance of the proposed laser sensor has been demonstrated to ensure simultaneous measurement with high-accuracy and good repeatability.

B. RH RESPONSE

During the RH and temperature experiment, the sensing probe including PVA-coated LPG and $UFBG_2$ was fixed into the climate chamber for realizing to monitor the change of the RH and temperature, and the other parts of the fiber laser system were fixed on the optical platform. For the RH measurement, the temperature was held at 25 °C. Fig. 6 shows the actual spectrum from 1540nm to 1565nm measured by OSA under 30% RH, 40% RH, 50% RH, 60% RH, 70% RH and 80% RH. The output power variations at the dual-wavelength laser peak are opposite with RH from 30% to 80%. At the same time, dual emission wavelengths basically remain constant.

Further, the response curve between RH and the proposed laser sensor has been investigated, as shown in Fig. 7. Because of external environment change and identical pump light jitter, the measurement of differential intensity at different wavelengths is used to remove the instability of laser sensor by above-mentioned factors. As can be acquired from Fig. 7(a), the RH function based on differential output power measurement from 30% to 85% is in a quadratic equation, and the quadratic and linear coefficient are 0.005 dB/%^{2} and −0.335 dB/% (R^2 approach to 0.995), respectively. Meanwhile, the laser sensor has a good linear relationship under high RH experiment from 55% to 85%, and the RH sensitivity

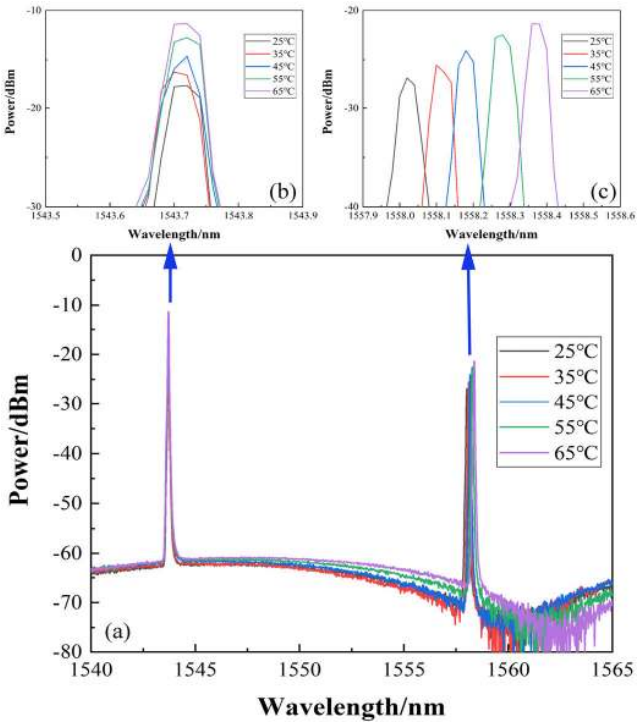

FIGURE 8. (a) Experimental laser spectral variation of proposed sensor as temperature from 25 °C to 65 °C; (b)(c) Local amplification diagram of laser peak location.

coefficient is 0.358 dB/% (R^2 approach to 0.997). Then, we have also researched the variation of wavelength difference at different RH. The wavelength difference basically remains constant, as shown in Fig. 7(b).

C. TEMPERATURE RESPONSE

Temperature cross-sensitivity is the main concern which needs consideration for such RH sensors. The temperature response of the proposed laser sensor was conducted and the actual spectral shift from 25 °C to 65 °C temperature was depicted in Fig. 8, when the RH was held at 50%.

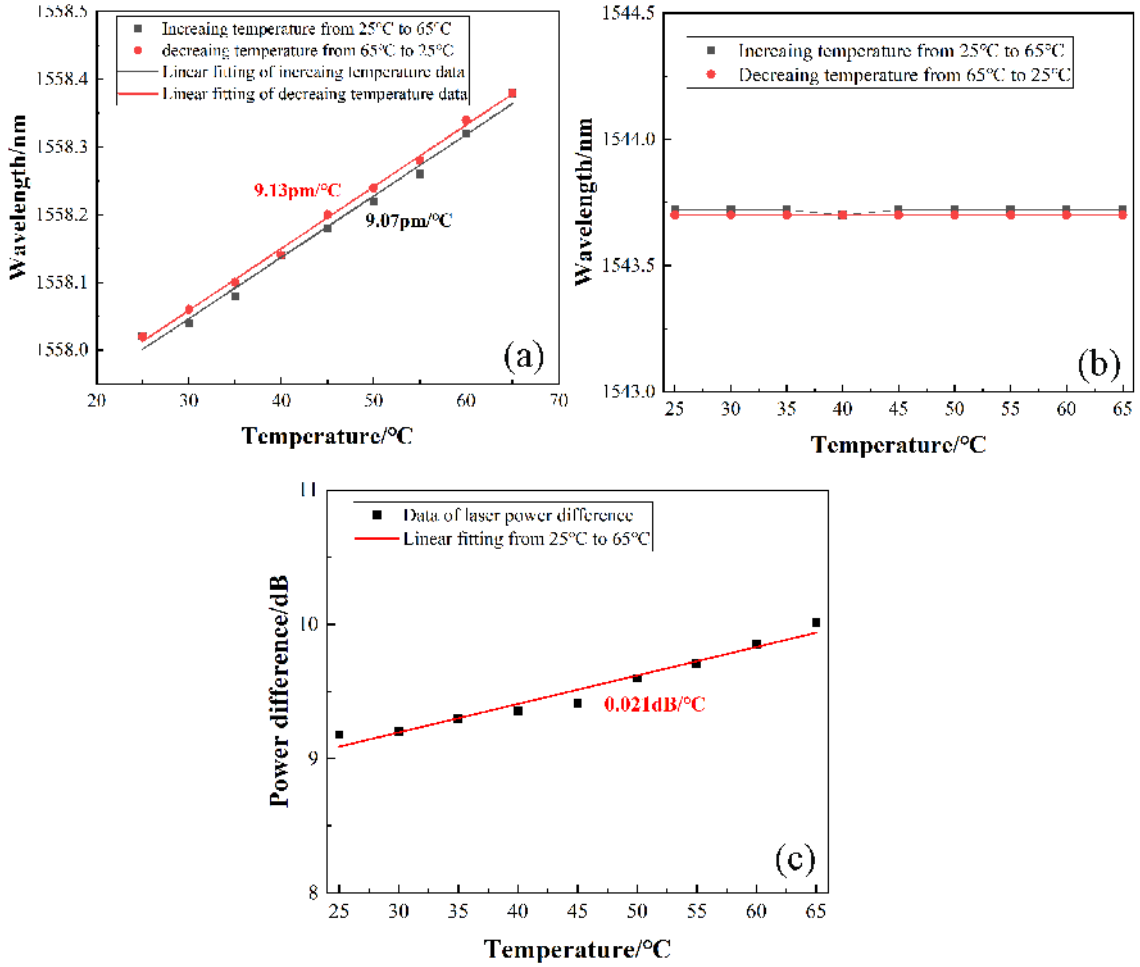

FIGURE 9. (a)(b) Each wavelength variation of the proposed laser sensor as temperature from 25 °C to 65 °C. (c) The change of differential output power intensity as temperature from 25 °C to 65 °C.

We can find that the output power at the dual-wavelength laser peak increases gradually with the temperature from 25 °C to 65 °C. Meanwhile, the peak wavelength of the dual-wavelength fiber laser at the $UFBG_2$ position presents red-shift, and the peak wavelength at the $UFBG_1$ position basically remains constant.

Furthermore, the results of the characterization for the dual-wavelength fiber laser sensor and the linear regression of the temperature response at different wavelengths and differential output power in the range from 25 °C to 65 °C are presented in Fig. 9. It can be seen that the temperature function based on lasing wavelength measurement and differential output power measurement show a good linear relation. At the same time, the measured experiment of temperature is repeated twice, and the two measurement results show good consistency. Then, the temperature sensitivity of 9.1pm/°C based on wavelength demodulation at the $UFBG_2$ position (R^2 approach to 0.991) is analyzed, and the temperature sensitivity at the $UFBG_1$ position approach to zero. Meanwhile, the temperature sensitivity of 0.021 dB/°C (R^2 approach to 0.955) using differential output power measurement is obtained.

Through the above theoretical analysis and experimental data processing, the coefficient matrix can be given by

$$\begin{bmatrix} \frac{\Delta\lambda_{laser}}{\Delta P_{laser}} \end{bmatrix} = \begin{bmatrix} K_{11} & 0 \\ K_{21} & K_{22} \end{bmatrix} \begin{bmatrix} \frac{\Delta T}{\Delta RH} \end{bmatrix} = \begin{bmatrix} 9.1\,nm/°C & 0 \\ 0.358\,dB/\% & 0.021\,dB/°C \end{bmatrix} \begin{bmatrix} \frac{\Delta T}{\Delta RH} \end{bmatrix} \quad (9)$$

Based on the above formula, the discrimination between RH and temperature by the detection of wavelength shift and differential power intensity variation has been realized.

In order to research the simultaneous response characteristics of the RH and temperature for the proposed laser sensor, we have also measured the laser spectral datum at 60% and 30 °C, 65% and 40 °C, 70% and 45 °C, 75% and 50 °C, 80% and 60 °C in Fig. 10. Based on the laser spectral data (5.025 dB and 14.32 nm) at 55% and 25 °C as reference points, the measured wavelength difference and the variation of differential power intensity are 6.735 dB and 14.38 nm, 8.744 dB and 14.46 nm, 10.526 dB and 14.50 nm, 12.565 dB and 14.54 nm, 14.69 dB and 14.64 nm, which are approximately equal to the calculation data (6.92 dB and 14.37 nm, 8.92 dB and 14.46 nm, 10.815 dB and 14.50 nm,

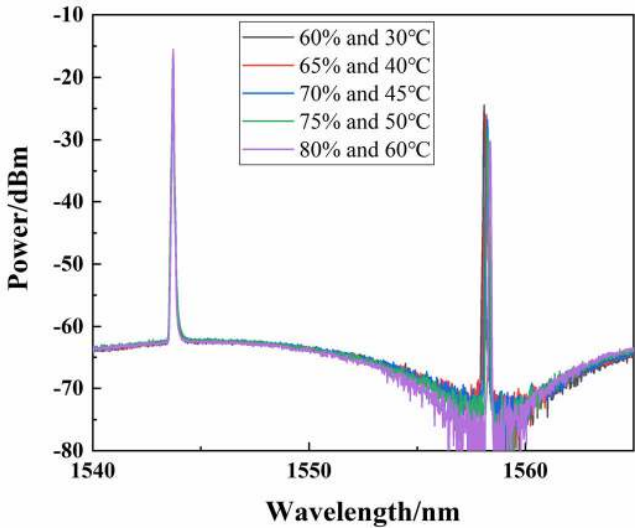

FIGURE 10. Experiemntal output spectral of the proposed fiber laser sensor at 60% and 30 °C, 65% and 40 °C, 70% and 45 °C, 75% and 50 °C, 80% and 60 °C.

12.71 dB and 14.55 nm, 14.71 dB and 14.64 nm) by formula 9. Thus, the dual-wavelength fiber laser sensor has potential applications in the RH and temperature simultaneous measurement with high SNR, high accuracy, good repeatability.

IV. CONCLUSION

A dual-wavelength fiber laser sensor for simultaneous detection of the RH and temperature is proposed and experimentally demonstrated. The PVA-coated LPG combines the $UFBG_2$ as the sensing probe, and the $UFBG_1$ is used as the reference grating. The RH and temperature can affect the variation of laser wavelength and output power intensity. Experimental results show that the RH function based on the differential output power measurement from 30% to 85% is in a quadratic equation, and the measured quadratic and linear coefficients are 0.005 dB/%^{2} and −0.335 dB/%. From 55% to 85%, the RH function shows a good linear relation and the RH sensitivity coefficient is 0.358 dB/%. At the same time, the temperature function based on lasing wavelength measurement and differential output power measurement all show good linear relation, and the temperature sensitivity coefficients are 9.1 pm/°C and 0.021 dB/°C. Compared to the conventional fiber-optic RH and temperature sensors, the proposed fiber laser sensing structure with high SNR, high accuracy, and good repeatability has the capability of simultaneous multi-parameter measurement.

REFERENCES

[1] X. Huang, B. Li, L. Wang, X. Lai, H. Xue, and J. Gao, "Superhydrophilic, underwater superoleophobic, and highly stretchable humidity and chemical vapor sensors for human breath detection," *ACS Appl. Mater. Interface*, vol. 11, no. 27, pp. 24533–24543, Jul. 2019.

[2] J. M. Arimi, E. Duggan, M. O'Sullivan, J. G. Lyng, and E. D. O'Riordan, "Effect of moisture content and water mobility on microwave expansion of imitation cheese," *Food Chem.*, vol. 121, no. 2, pp. 509–516, Jul. 2010.

[3] L. Alwis, T. Sun, and K. T. V. Grattan, "[INVITED] developments in optical fibre sensors for industrial applications," *Opt. Laser Technol.*, vol. 78, pp. 62–66, Apr. 2016.

[4] C.-L. Lee, Y.-W. You, J.-H. Dai, J.-M. Hsu, and J.-S. Horng, "Hygroscopic polymer microcavity fiber Fizeau interferometer incorporating a fiber Bragg grating for simultaneously sensing humidity and temperature," *Sens. Actuators B, Chem.*, vol. 222, pp. 339–346, Jan. 2016.

[5] R. Oliveira, L. Bilro, T. H. R. Marques, C. M. B. Cordeiro, and R. Nogueira, "Simultaneous detection of humidity and temperature through an adhesive based Fabry–Pérot cavity combined with polymer fiber Bragg grating," *Opt. Lasers Eng.*, vol. 114, pp. 37–43, Mar. 2019.

[6] G. Woyessa, J. K. M. Pedersen, A. Fasano, K. Nielsen, C. Markos, H. K. Rasmussen, and O. Bang, "Zeonex-PMMA microstructured polymer optical FBGs for simultaneous humidity and temperature sensing," *Opt. Lett.*, vol. 42, no. 6, pp. 1161–1164, Mar. 2017.

[7] G. Yan, Y. Liang, E.-H. Lee, and S. He, "Novel knob-integrated fiber Bragg grating sensor with polyvinyl alcohol coating for simultaneous relative humidity and temperature measurement," *Opt. Express*, vol. 23, no. 12, pp. 15624–15634 , Jun. 2015.

[8] J. Yang, X. Dong, K. Ni, C. C. Chan, and P. P. Shun, "Intensity-modulated relative humidity sensing with polyvinyl alcohol coating and optical fiber gratings," *Appl. Opt.*, vol. 54, no. 10, pp. 2620–2624, Apr. 2015.

[9] J. Shi, D. Xu, and W. Xu, "Humidity sensor based on Fabry–Pérot interferometer and intracavity sensing of fiber laser," *J. Lightw. Technol.*, vol. 35, no. 21, pp. 4789–4795, Nov. 1, 2017.

[10] S. Zhang, X. Dong, T. Li, C. C. Chan, and P. P. Shum, "Simultaneous measurement of relative humidity and temperature with PCF-MZI cascaded by fiber Bragg grating," *Opt. Commun.*, vol. 303, pp. 42–45, Aug. 2013.

[11] W. Bai, M. Yang, J. Dai, H. Yu, G. Wang, and C. Qi, "Novel polyimide coated fiber Bragg grating sensing network for relative humidity measurements," *Opt. Express*, vol. 24, no. 4, pp. 3230–3237, Feb. 2016.

[12] M. Consales, G. Berruti, A. Borriello, M. Giordano, S. Buontempo, G. Breglio, A. Makovec, P. Petagna, and A. Cusano, "Nanoscale TiO_2-coated LPGs as radiation-tolerant humidity sensors for high-energy physics applications," *Opt. Lett.*, vol. 39, no. 14, pp. 4128–4131, Jul. 2014.

[13] M. R. K. Soltanian, A. S. Sharbirin, M. M. Ariannejad, I. S. Amiri, R. M. De La Rue, G. Brambilla, B. M. A. Rahman, K. T. V. Grattan, and H. Ahmad, "Variable waist-diameter Mach–Zehnder tapered-fiber interferometer as humidity and temperature sensor," *IEEE Sensors J.*, vol. 16, no. 15, pp. 5987–5992, Aug. 2016.

[14] G. Berruti, M. Consales, M. Giordano, L. Sansone, P. Petagna, S. Buontempo, G. Breglio, and A. Cusano, "Radiation hard humidity sensors for high energy physics applications using polyimide-coated fiber Bragg gratings sensors," *Sens. Actuators B, Chem.*, vol. 177, pp. 94–102, Feb. 2013.

[15] C.-T. Ma, Y.-W. Chang, Y.-J. Yang, and C.-L. Lee, "A dual-polymer fiber Fizeau interferometer for simultaneous measurement of relative humidity and temperature," *Sensors*, vol. 17, no. 11, p. 2659, 2017.

[16] S. Wu, G. Yan, Z. Lian, X. Chen, B. Zhou, and S. He, "An open-cavity Fabry–Pérot interferometer with PVA coating for simultaneous measurement of relative humidity and temperature," *Sens. Actuators B, Chem.*, vol. 225, pp. 50–56, Mar. 2016.

[17] B. Yin, M. Wang, S. Wu, Y. Tang, S. Feng, Y. Wu, and H. Zhang, "Fiber ring laser based on MMF-PMFBG-MMF filter for three parameters sensing," *Opt. Express*, vol. 25, no. 25, pp. 30946–30955, Dec. 2017.

[18] X. Yang, S. Bandyopadhyay, L.-Y. Shao, D. Xiao, G. Gu, and Z. Song, "Side-polished DBR fiber laser with enhanced sensitivity for axial force and refractive index measurement," *IEEE Photon. J.*, vol. 11, no. 3, pp. 1–10, Jun. 2019.

[19] L.-Y. Shao, J. Liang, X. Zhang, X. Zou, B. Luo, W. Pan, and Y. Lianshan, "High resolution refractive index sensing with dual-wavelength fiber laser," *IEEE Sensors J.*, to be published.

[20] B. Yin, S. Wu, M. Wang, W. Liu, H. Li, B. Wu, and Q. Wang, "High-sensitivity refractive index and temperature sensor based on cascaded dual-wavelength fiber laser and SNHNS interferometer," *Opt. Express*, vol. 27, no. 1, pp. 252–264, Jan. 2019.

[21] X. Yang, L. Duan, H. Zhang, Y. Lu, G. Wang, and J. Yao, "Highly sensitive dual-wavelength fiber ring laser sensor for the low concentration gas detection," *Sens. Actuators B, Chem.*, vol. 296, Oct. 2019, Art. no. 126637.

[22] J. A. Martin-Vela, J. M. Sierra-Hernandez, A. Martinez-Rios, J. M. Estudillo-Ayala, E. Gallegos-Arellano, D. Toral-Acosta, T. E. Porraz-Culebro, and D. Jauregui-Vazquez, "Curvature sensing setup based on a fiber laser and a long-period fiber grating," *IEEE Photon. Technol. Lett.*, vol. 31, no. 15, pp. 1265–1268, Aug. 1, 2019.

[23] Y. Dai, Q. Sun, S. Tan, J. Wo, J. Zhang, and D. Liu, "Highly sensitive liquid-level sensor based on dual-wavelength double-ring fiber laser assisted by beat frequency interrogation," *Opt. Express*, vol. 20, no. 25, pp. 27367–27376, Dec. 2012.
[24] D. Lo Presti, C. Massaroni, and E. Schena, "Optical fiber gratings for humidity measurements: A review," *IEEE Sensors J.*, vol. 18, no. 22, pp. 9065–9074, Nov. 2018.
[25] L. Alwis, T. Sun, and K. T. V. Grattan, "Design and performance evaluation of polyvinyl alcohol/polyimide coated optical fibre grating-based humidity sensors," *Rev. Sci. Instrum.*, vol. 84, no. 2, Feb. 2013, Art. no. 025002.
[26] T. Erdogan, "Fiber grating spectra," *J. Lightw. Technol.*, vol. 15, no. 8, pp. 1277–1294, Aug. 1997.
[27] A. M. Vengsarkar, P. J. Lemaire, J. B. Judkins, V. Bhatia, T. Erdogan, and J. E. Sipe, "Long-period fiber gratings as band-rejection filters," *J. Lightw. Technol.*, vol. 14, no. 1, pp. 58–65, Jan. 1996.
[28] S. W. James and R. P. Tatam, "Optical fibre long-period grating sensors: Characteristics and application," *Meas. Sci. Technol.*, vol. 14, no. 5, pp. R49–R61, May 2003.
[29] V. Bhatia, "Applications of long-period gratings to single and multi-parameter sensing," *Opt. Express*, vol. 4, no. 11, pp. 457–466, May 1999.
[30] H. Liu, H. Liang, M. Sun, K. Ni, and Y. Jin, "Simultaneous measurement of humidity and temperature based on a long-period fiber grating inscribed in fiber loop mirror," *IEEE Sensors J.*, vol. 14, no. 3, pp. 893–896, Mar. 2014.
[31] O. Frazão, L. A. Ferreira, F. M. Araújo, and J. L. Santos, "Applications of fiber optic grating technology to multi-parameter measurement," *Fiber Integr. Opt.*, vol. 24, nos. 3–4, pp. 227–244, May 2005.
[32] S. Wang, S. Liu, W. Ni, S. Wu, and P. Lu, "Dual-wavelength highly-sensitive refractive index sensor," *Opt. Express*, vol. 25, no. 13, pp. 14389–14396, Jun. 2017.

BIN YIN received the B.S. and Ph.D. degrees from Beijing Jiaotong University, in 2011 and 2016, respectively. He has carried out Postdoctoral research with the Ocean University of China, from 2016 to 2019. He is currently an Associate Professor with the College of Information Science and Engineering, Ocean University of China. His research interests include fiber-optic sensing technology, fiber devices, microwave photonics, and environmental monitoring.

GUOFENG SANG is currently pursuing the bachelor's degree with the Ocean University of China. His research interests include fiber optic sensor and fiber laser.

RAN YAN is currently pursuing the bachelor's degree with the Ocean University of China. His research interests include fiber optic sensor and biomedical sensing.

YUHENG WU is currently pursuing the bachelor's degree with the Ocean University of China. His research interest includes fiber optic sensor.

SONGHUA WU received the Ph.D. degree from the Ocean University of China, in 2004. He is currently a Professor with the College of Information Science and Engineering, Ocean University of China. His current research interests include laser detection technology and its applications in ocean atmospheric dynamics and environmental monitoring.

MUGUANG WANG (Member, IEEE) received the Ph.D. degree from Beijing Jiaotong University, in 2004. He is currently a Professor with the Institute of Lightwave Technology, Beijing Jiaotong University. His current research interests include microwave photonics, fiber sensing, and high-speed optical fiber communication systems.

WENQI LIU received the B.S. degree from Beijing Jiaotong University, in 2011, and the Ph.D. degree from the National Center for Nanoscience and Technology, in 2016. From 2016 to 2019, she has carried out postdoctoral research with the Qingdao Institute of Bioenergy and Bioprocess Technology, Chinese Academy of Sciences, where she is currently working. Her main research interest includes electrochemical sensor.

HAISU LI received the Ph.D. degree from Beijing Jiaotong University, in 2017. He is currently an Associate Professor with Beijing Jiaotong University. His current research focuses on developing photonic structures-based waveguide devices for both optical communications and terahertz applications.

QICHAO WANG received the B.S. degree from the Ocean University of China, in 2013, where he is currently pursuing the Ph.D. degree. His current research interest includes optical detection of atmosphere and ocean.